

Reactivity Modes of an Iron Bis(alkoxide) Complex with Aryl Azides: Catalytic Nitrene Coupling vs Formation of Iron(III) Imido Dimers

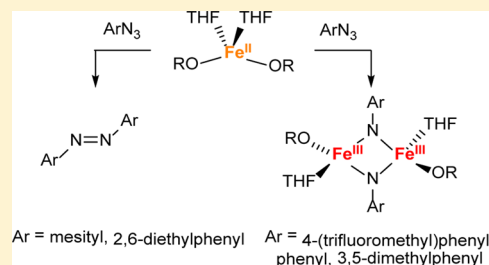
James A. Bellow,[†] Maryam Yousif,[†] Alyssa C. Cabelof,[‡] Richard L. Lord,[‡] and Stanislav Groysman^{*,†}

[†]Department of Chemistry, Wayne State University, 5101 Cass Avenue, Detroit, Michigan 48202, United States

[‡]Department of Chemistry, Grand Valley State University, Allendale, Michigan 49401, United States

S Supporting Information

ABSTRACT: The iron bis(alkoxide) complex $\text{Fe}(\text{OR})_2(\text{THF})_2$ ($\text{R} = \text{C}^t\text{Bu}_2\text{Ph}$), **1**, was found to have strikingly different reactivity with various aryl azides, ArN_3 . Azides with methyl or ethyl groups in the *ortho* positions of the phenyl ring react catalytically via nitrene coupling to give azoarenes, $\text{ArN}=\text{NAr}$. Catalyst loading as low as 1 mol % yields clean, quantitative conversion of aryl azides to azoarenes at room temperature in as little as 4 h. A combination of two different aryl azides leads to the catalytic formation of all three possible azoarenes, including the asymmetric one. In contrast, reactions with aryl azides lacking *ortho* substituents yield stable dimeric iron imido complexes of the form $(\text{RO})(\text{THF})\text{Fe}(\mu\text{-NAr})_2\text{Fe}(\text{THF})(\text{OR})$ ($\text{Ar} = 4$ - (trifluoromethyl)phenyl, **5**; $\text{Ar} = \text{phenyl}$, **6**; $\text{Ar} = 3,5$ -dimethylphenyl, **7**), which do not undergo catalytic nitrene coupling. The isocyanide adduct $\text{Fe}(\text{OR})_2(\text{CNR})_2$ (**4**, $\text{R} = 2,6$ -dimethylphenyl) was obtained from the reaction of $\text{Fe}(\text{OR})_2(\text{THF})_2$ with two equivalents of isocyanide. No C–N bond formation was observed in the reaction of compound **4** with azides or in the reaction of compounds **5**–**7** with isocyanides.



INTRODUCTION

Azoarenes are highly colored photoresponsive compounds that have found various industrial uses as food and textile dyes, as well as chemical indicators.^{1,2} In addition, azoarenes have been investigated for their utilization in optical storage devices,³ liquid crystal displays,⁴ molecular switches,⁵ and drug delivery.⁶ Common routes to the formation of azoarenes include azo coupling via a diazonium intermediate, as well as the Mills and Wallach reactions.⁷ Catalytic transition metal-mediated formation of azoarenes from azides may be beneficial to the existing stoichiometric methods, as they lead to the desired product in one step, with dinitrogen as the sole byproduct. Middle to late transition metal complexes are particularly useful vehicles for the formation of nitrene from azides and its subsequent transfer.⁸ Transition metal-catalyzed nitrene transfer reactions often result in the amination of alkanes and aziridination of olefins.^{9,10} However, while stoichiometric nitrene coupling has been reported by several groups,¹¹ catalytic formation of azoarenes via transition metal catalysts is rare.¹²

We are investigating the reactivity of earth-abundant 3d metal centers in bis(alkoxide) ligand environments. We have recently reported the synthesis of an iron(II) complex in a bis(alkoxide) ligand environment, $\text{Fe}(\text{OR})_2(\text{THF})_2$ ($\text{R} = \text{C}^t\text{Bu}_2\text{Ph}$) (**1**).¹³ We have also demonstrated that compound **1** is a highly reactive species capable of reductively coupling adamantyl azide to form the bridging hexazene complex $(\text{RO})_2\text{Fe}(\mu\text{-}\kappa^2\text{-AdN}_6\text{Ad})\text{Fe}(\text{OR})_2$ (Figure 1).^{13b} Such reactivity has been previously observed only with strongly reducing Fe(I), Mg(I), or Zn(I) systems.¹⁴ The unusual reactivity of **1**

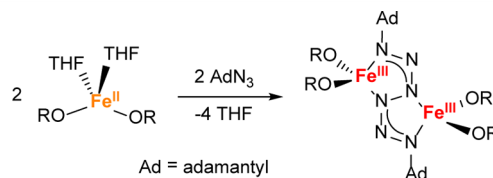


Figure 1. Reaction of **1** with adamantyl azide forming the bridging hexazene complex $(\text{RO})_2\text{Fe}(\mu\text{-}\kappa^2\text{-AdN}_6\text{Ad})\text{Fe}(\text{OR})_2$.^{13b}

with an alkyl azide prompted us to next investigate its reactivity with aryl azides. Herein we report that **1** is capable of forming both symmetric and asymmetric azoarenes catalytically and selectively from aryl azides featuring two *ortho* substituents. We also isolate three bridging Fe(III)-imide dimers, as well as the reaction byproduct $\text{Fe}(\text{OR})_3$, and propose a possible mechanism that leads to these products.

RESULTS AND DISCUSSION

The addition of one equivalent of mesityl azide to **1** in toluene led to immediate gas evolution and a gradual color change to dark orange (Figure 2). Upon reaction workup, two different orange products cocrystallized. The first product, as observed by X-ray diffractometry, was the iron(III) tris(alkoxide) complex $\text{Fe}(\text{OR})_3$, **2**, a rare example of iron in a trigonal planar coordination environment.¹⁵ The second product, also identified by X-ray crystallography, was azomesitylene,

Received: March 19, 2015

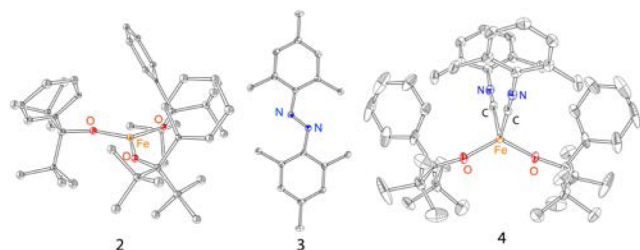
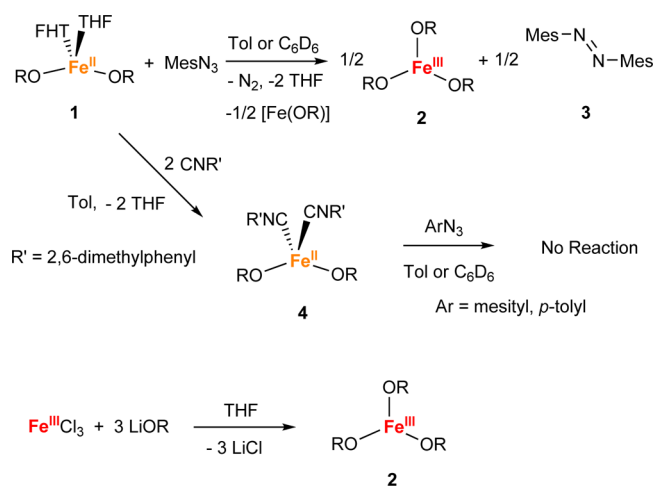


Figure 2. (Top) Stoichiometric reaction of $\text{Fe}(\text{OR})_2(\text{THF})_2$ (1) with mesityl azide yielding $\text{Fe}(\text{OR})_3$ (2) and azomesitylene (3); independent synthesis of $\text{Fe}(\text{OR})_3$; synthesis of $\text{Fe}(\text{OR})_2(\text{CNR}')_2$ (4). (Bottom) X-ray crystal structures of the obtained products 2–4 (40% probability ellipsoids). Selected bond distances (Å) and angles (deg) for 2: Fe–O, 1.816(1); O–Fe–O, 119.99(2). Selected bond distances (Å) and angles (deg) for 4: Fe–O, 1.833(3); Fe–C, 2.085(4); O–Fe–O, 125.5(2).

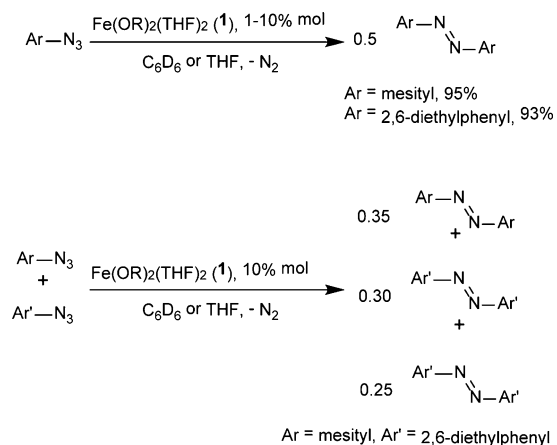
MesNNMes, 3. Running the same reaction in C_6D_6 and taking NMR of the resulting dark orange solution (in the presence of an internal standard) revealed quantitative consumption of the starting azide, as well as three new peaks corresponding to a new product featuring a mesityl group, consistent with the formation of 3. Thus, both X-ray crystallography and NMR spectroscopy indicate that instead of reductive coupling of the aryl azide to form hexazene, nitrene formation occurs followed by the subsequent N–N coupling to form an azoarene. ^1H NMR spectroscopy indicates that azoarene forms quantitatively. We were not able to determine the yield of complex 2 ($\text{Fe}(\text{OR})_3$) due to its nearly featureless NMR and UV–vis spectra. Complex 2 can be independently synthesized from the reaction of an Fe(III) source, FeCl_3 , with three equivalents of LiOR (Figure 2).

We have investigated the reactivity of the transient nitrene functionality toward activation of a weak C–H bond (of cyclohexadiene) and N–C bond formation with an isocyanide (2,6-dimethylphenyl isocyanide). The reaction appears to be highly preferential toward nitrene coupling versus C–H bond activation: on running the reaction in cyclohexadiene as a solvent, only the azoarene product is observed by NMR, with no evidence of C–H activation. To test for the possible C–N bond formation, we have studied the reactivity of the $\text{Fe}(\text{OR})_2(\text{THF})_2$ /azide mixture in the presence of an isocyanide. Addition of a 1:1 mixture of isocyanide and mesityl azide to a solution of 1 in C_6D_6 leads to the formation of a green solution. No azoarene formation is detected, and no

other new peaks are visible in the NMR, but the isocyanide peaks disappear completely, presumably due to isocyanide coordination to the metal. To examine this hypothesis, we have independently synthesized the isocyanide adduct $\text{Fe}(\text{OR})_2(\text{CNR}')_2$ (4). Green $\text{Fe}(\text{OR})_2(\text{CNR}')_2$ was obtained by the addition of two equivalents of the isocyanide to the solution of complex 1 in toluene and characterized by X-ray diffraction (Figure 2), ^1H NMR spectroscopy, and IR spectroscopy. We next treated a C_6D_6 solution of 4 with mesityl azide or phenyl azide. ^1H NMR spectroscopy demonstrates that no reaction between 4 and mesityl/phenyl azide takes place.

Nitrene coupling was also found to be catalytic (Scheme 1). Using 1–10% catalyst loading, mesityl azide was cleanly

Scheme 1. Catalytic Formation of Azoarenes from Aryl Azides Using $\text{Fe}(\text{OR})_2(\text{THF})_2$ (1)



converted to azomesitylene (see Table S1). NMR spectroscopy in the presence of an internal standard demonstrates that the conversion is nearly quantitative; pure azomesitylene was isolated in 95% yield using 1 mol % catalyst. Similar catalytic conversion of 2,6-diethylphenyl azide to the corresponding azoarene is also possible. NMR monitoring of the reaction mixture demonstrates full conversion within 24 h. Pure azo(2,6-diethylbenzene) was isolated in 93% yield at 5 mol % catalyst. In addition to the symmetric coupling products, we also demonstrate that asymmetric coupling is possible with our system. Using an equal number of equivalents of mesityl azide and 2,6-diethylphenyl azide with 10% catalyst loading led to catalytic formation of all three possible azoarene products in similar quantities, as confirmed by NMR yield (35% of azomesitylene, 30% of the mixed azoarene, and 25% of azo(2,6-diethylphenylbenzene)). All symmetric and asymmetric azoarenes were identified by NMR spectroscopy and mass spectrometry. Control experiments indicate that $\text{Fe}(\text{OR})_2(\text{THF})_2$ is essential for the catalytic or stoichiometric nitrene formation. No azide consumption or azoarene formation was observed when $\text{Fe}(\text{OR})_2(\text{THF})_2$ was replaced by FeCl_2 or FeCl_3 or in the absence of any iron catalyst.

Surprisingly, reducing the steric bulk of the aryl azide to *para*-tolyl or *ortho*-tolyl groups yielded no azoarene formation, even at elevated temperatures, as evidenced by NMR. However, a color change to red-brown and gas evolution were observed in both cases, implying formation of metal-imido species. Similarly, no azoarene formation was observed in the reaction with the more electron-rich aryl azide azidoanisole or for the

electron-poor 4-(trifluoromethyl)phenyl azide. Thus, we suggest that the azoarene formation in our system is governed by a steric effect: the presence of the two R groups in the *ortho* positions is required for catalysis. To determine the product formed in the reaction with the sterically unhindered azides, a stoichiometric reaction of **1** with 4-(trifluoromethyl)phenyl azide was attempted. Crystallization led to the isolation of black crystals confirmed to be the iron mono(alkoxide) dimer (RO)(THF)Fe(μ -NAr)₂Fe(OR)(THF) (Ar = 4-(trifluoromethyl)phenyl), **5**, possessing two bridging imido moieties (Figure 3). The Fe₂(μ -NAr)₂ diamond core motif

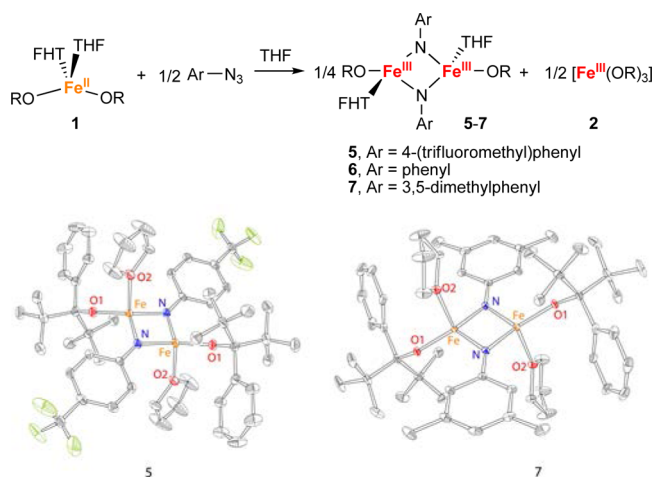


Figure 3. (Top) Reaction of Fe(OR)₂(THF)₂ (**1**) with aryl azides yielding (RO)(THF)Fe(μ -NAr)₂Fe(OR)(THF) (**5**–**7**). (Bottom) X-ray crystal structures of compounds **5** (left) and **7** (right) (40% probability ellipsoids). Selected bond distances (Å) and angles (deg) for **5**: Fe–N, 1.881(3)/1.897(3); Fe–O1, 1.803(2); Fe–O2, 2.075(2); N–Fe–N, 96.03(6); O1–Fe–O2, 102.58(2). Selected bond distances (Å) and angles (deg) for **7**: Fe–N, 1.875(1)/1.902(1); Fe–O1, 1.833(1); Fe–O2, 2.085(1); N–Fe–N, 96.03(6); O1–Fe–O2, 102.58(2).

depicted in the crystal structure of **5** is rare in diiron species, but cluster compounds containing several iron centers with bridging aryl imidos are more numerous.¹⁶ Analogous bis(imido) products were isolated using the smaller phenyl azide (**6**) and 3,5-dimethylphenyl azide (**7**). Crystals suitable for X-ray diffraction could not be isolated for complex **6**, but elemental analysis confirms the identity of the bulk product. Crystals of the bis(imido) complex **7** were also obtained (Figure 3). We note that the structures of **5** and **7** are consistent with the Fe(III) oxidation state, as indicated by the Fe–OR bond distances and the presence of the Fe₂(μ -NAr)₂ core (observed only for Fe(III) in previously synthesized complexes).^{15b,16d–g} The structures of both **5** and **7** are centrosymmetric, containing only half of the complex in the asymmetric unit. Two distinct, albeit very close, Fe–N bonds are observed (see Figure 3 for details). The observed Fe–Fe distances of 2.543(1) Å (**5**) and 2.5268(4) Å (**7**) are closely related to the Fe–Fe distances in the previously reported (NHC)(X)Fe(μ -NAr)₂Fe(NHC)(X) complexes, which were in the 2.424(4)–2.527(1) Å range (NHC = N-heterocyclic carbene, X = Cl, F).^{16g} We postulate that the formation of **5**–**7**, containing iron mono(alkoxide) centers, is accompanied by the formation of the iron tris(alkoxide) complex **2**. Formation of compound **2** as a byproduct was observed in the stoichiometric and catalytic coupling of azoarenes (see

above). Unfortunately, we were not able to detect **2** in the reaction mixtures due to its relatively featureless UV–vis and NMR spectra, as well as its overall instability.

Complexes **5**–**7** appear to be stable molecules that are unreactive toward additional equivalents of azide. After treating compound **7** with an excess of mesityl azide and stirring for 24 h, no color change was observed, and no new peaks appeared in the ¹H NMR spectrum. The reaction of compound **6** with 2,6-dimethylphenyl isocyanide gave similar results. Additionally, heating a solution of **7** to 50 °C for 4 h in an attempt to force formation of the azoarene led to no reaction.

The mechanism to rationalize formation of the compounds described in the paper is presented in Figure 4. Initial

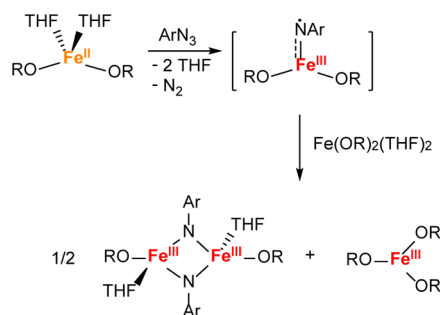


Figure 4. Proposed “comproportionation” reaction explaining formation of the iron-imido dimers and Fe(OR)₃.

coordination of the azide to the metal followed by dinitrogen extrusion leads to the formation of the reactive iron imido intermediate Fe(OR)₂(NAr). We were not able to directly observe Fe(OR)₂(NAr); however, we shed light on its electronic structure by DFT calculations (see below). We also note that a compound similar to Fe(OR)₂(NAr) was proposed in other systems.^{17,18} Specifically, an iron(IV) imido complex was postulated as an intermediate on the route to intramolecular C–H activation using adamantyl azide in the similar bis(aryloxy) system Fe(OC₆H₂-2,6-Ad-4-R)₂ (R = Me, ⁱPr).¹⁹ The postulated intermediate Fe(OR)₂(NAr) is strongly oxidizing and reacts with one equivalent of the reducing Fe(II) bis(alkoxide) complex **1** in a comproportionating fashion to yield two iron(III) complexes. One of them is the iron(III) tris(alkoxide) complex **2**, and the other is the iron(III) mono(alkoxide) imido dimer (RO)(THF)Fe(μ -NAr)₂Fe(OR)(THF). It is possible that the formation of the dimer (RO)(THF)Fe(μ -NAr)₂Fe(OR)(THF) is preceded by the formation of the monomer Fe(OR)(NAr)(THF); however, we were not able to obtain any evidence to this end. Both Fe(OR)₂(NAr) and (RO)(THF)Fe(μ -NAr)₂Fe(OR)(THF) can be responsible for the observed catalytic nitrene coupling, via either a mononuclear (as previously described by Hillhouse and proposed in the reaction mechanism by Peters)^{10f,12b} or dinuclear mechanism (coupling of bridging imidos). Kinetic experiments demonstrate that the reaction appears to be of second order in the azide (see Figures S31–35); this finding may be consistent with both mechanisms. To elucidate the reaction order in Fe, we attempted the initial rate method, in which we changed the concentration of the iron precursor while following the decrease in the concentration of the azide. However, several different measurements did not lead to a definitive integer rate. It is possible that several mechanisms are responsible for the nitrene coupling in our system, and the

prevalence of the given mechanism is determined by the concentration of the iron species.

To better understand the electronic structure of the putative intermediate $\text{Fe}(\text{OR})_2(\text{NAr})$, it was explored using DFT at the B3LYP/6-311G(d) level of theory.²⁰ Spin states ranging from singlet to septet were optimized, and the high-spin quintet state was found to be lowest in energy. B3LYP is documented to overstabilize high-spin states due to its parametric dependence on the amount of Hartree–Fock exchange,²¹ so single-point energies at the optimized B3LYP structures were performed with OPBE,²² a functional known to produce accurate spin-state splittings.²³ The quintet was still the lowest energy spin state with OPBE (Table S7). In principle, this quintet species should be high-spin Fe^{IV} with two OR^- and one NAr^{2-} ligands and therefore should only exhibit α spin density at the metal. The computed spin density is shown in Figure 5. In addition to

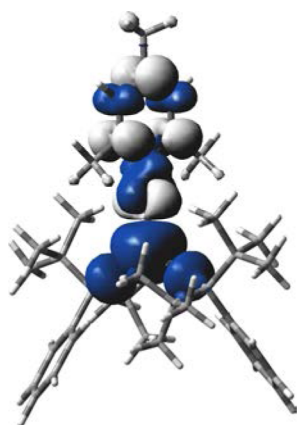


Figure 5. Spin density isosurface plot (iso = 0.002 au) for quintet $\text{Fe}(\text{OR})_2(\text{NAr})$.

α spin density at the Fe center, there is significant β spin density on the NAr ligand. A corresponding orbital analysis (Table S4) showed five α electrons at Fe with weak overlap between a $d-\pi$ orbital ($S\alpha\beta \sim 0.53$) and a NAr π orbital, which suggests this species is best described as a high-spin Fe^{III} antiferromagnetically coupled to NAr^{\bullet} . This description is consistent for OPBE, which does not have explicit exchange and therefore should not overstabilize an electronic configuration with maximal exchange (d^5) at the metal center. It is worth noting, however, that all of the states considered have spin contamination and must be interpreted with caution. Our formulation of the electronic structure of $\text{Fe}(\text{OR})_2(\text{NAr})$ is consistent with previous calculations by Betley and co-workers on high-spin Fe-imido species, which found Fe to be $\text{Fe}(\text{III})$ AF-coupled with an imido radical.^{10h} However, we note that while DFT describes our $\text{Fe}(\text{OR})_2(\text{NAr})$ species as an imido radical, it did not activate a CH bond, unlike Betley's system.

SUMMARY

We have discovered a new catalyst capable of performing the rare nitrene coupling to form azoarenes. To the best of our knowledge, this is the first example of a nitrene-coupling precatalyst that contains an $\text{Fe}(\text{II})$ center, as previous examples included $\text{Fe}(\text{I})$ or $\text{Ru}(\text{I})$ complexes. We demonstrated that the iron bis(alkoxide) **1** selectively converts aryl azides with steric bulk in the *ortho* positions catalytically to yield clean azoarenes in high yield. For nonbulky aryl azides, formation of the unreactive bridging imido species **5–7** was observed. Our

future work will focus on the catalytic formation of additional diazenes with a particular focus on the diazenes that could be used as dyes and on the further investigation of the reaction mechanism.

EXPERIMENTAL SECTION

General Methods and Procedures. All reactions involving air-sensitive materials were executed in a nitrogen-filled glovebox. The syntheses of the lithium salt of the ligand and the iron bis(alkoxide) complex **1** were reported previously.¹³ Thallium(I) hexafluorophosphate was purchased from Strem. Mesityl azide,²⁴ 2,6-diethylphenyl azide,²⁵ and 3,5-dimethylphenyl azide²⁶ were synthesized according to literature procedures. All other materials were used as purchased from Aldrich. All solvents were purchased from Fisher Scientific and were of HPLC grade. The solvents were purified using an MBraun solvent purification system and stored over 3 Å molecular sieves. The complexes were characterized using NMR and IR spectroscopies, mass spectrometry, X-ray crystallography, elemental analysis, and the Evans method. NMR spectra were recorded at the Lumigen Instrument Center (Wayne State University) on a Varian Mercury 400 MHz NMR spectrometer in C_6D_6 at room temperature. IR spectra of powdered samples were recorded on a Shimadzu IR Affinity-1 FT-IR spectrometer outfitted with a MIRacle10 attenuated total reflectance accessory with a monolithic diamond crystal stage and pressure clamp. UV–visible spectra were obtained on a Shimadzu UV-1800 spectrometer. Low-resolution mass spectra were obtained on a Shimadzu LCMS 2020 using a 1:1 mixture of acetonitrile and water as the eluent, with 0.1% formic acid added. Elemental analyses were performed by Midwest Microlab LLC and Galbraith Laboratories Inc.

Synthesis and Characterization of Metal Complexes.

Stoichiometric Reaction of $\text{Fe}(\text{OR})_2(\text{THF})_2$ (1**) with Mesityl Azide.** A 5.0 mL toluene solution of mesityl azide (7.9 mg, 0.0488 mmol) was added dropwise to a 5.0 mL toluene solution of **1** (31.2 mg, 0.0488 mmol), leading to a gradual color change from yellow to a dark red-orange. Gas evolution was also observed. The reaction was stirred for 1 h, upon which the volatiles were removed in vacuo to give a red-orange residue. This residue was dissolved in a minimum amount of hexane and placed in the freezer. After 24 h, two different types of orange crystals had formed. The products (characterized by X-ray crystallography) were determined to be the iron tris(alkoxide), **2**, and the azoarene MesNNMes, **3**. An analogous experiment was run in C_6D_6 in the presence of 1,3,5-trimethoxybenzene as an internal standard. After stirring the reaction for 4 h, NMR revealed total consumption of the starting azide, with **3** as the only NMR-active product, formed in near-quantitative (96%) yield.

Preparation of $\text{Fe}(\text{OR})_3$ (2**) Using an $\text{Fe}(\text{III})$ Precursor.** A 5.0 mL THF solution of the lithium salt of the ligand LiOR (62.1 mg, 0.275 mmol) was prepared, along with a 5.0 mL THF solution of FeCl_3 (14.9 mg, 0.0915 mmol). The ligand salt was added to the metal chloride with stirring, upon which the solution color changed from yellow to orange. After stirring for 15 min, a THF solution of TlPF₆ (63.9 mg, 0.275 mmol) was added dropwise, leading to immediate formation of a white precipitate. The reaction was stirred for an hour, upon which the precipitate was filtered off, and the volatiles from the remaining filtrate were removed in vacuo to give an orange residue. This residue was redissolved in a minimum amount of hexane and placed in the freezer to afford orange crystals (52.9 mg, 63%). IR (cm^{-1}): 2974 (m), 2873 (m), 1558 (m), 1485 (w), 1386 (m), 1155 (w), 1053 (s), 1018 (m), 901 (w), 769 (m), 745 (w). $\mu_{\text{eff}} = 6.3 \mu\text{B}$ (calcd 5.9). $\lambda_{\text{max}} (\epsilon_{\text{M}})$: 317 (10 823), 519 (656). The compound was also characterized by X-ray crystallography. Anal. Calcd for $\text{C}_{45}\text{H}_{69}\text{O}_3\text{Fe}$: C, 75.7; H, 9.7. Found: C, 73.8; H, 9.6. The compound is unstable at room temperature, even under an inert atmosphere. After 24 h at room temperature in the solid state, orange crystals of compound **2** deform into an oily, dark green-brown residue. ¹H NMR of this green-brown residue reveals the presence of decomposed ligand. Even submitting a single crystal of this complex for elemental analysis under dry ice did not yield satisfactory elemental analysis results.

$Fe(OR)_2(CNAr)_2$ (**4**). To a stirred toluene solution of the iron bis(alkoxide) **1** (60.3 mg, 0.09 mmol) was added a toluene solution of 2,6-dimethylphenyl isocyanide (24.8 mg, 0.19 mmol) in one portion. Immediately the solution color changed to green. The reaction was stirred for 1 h, upon which the volatiles were removed in vacuo. The resulting green residue was dissolved in a minimum amount of hexane, filtered, and placed in the freezer to afford green X-ray quality crystals (42.0 mg, 59%). IR (cm^{-1}): 2978 (m), 2955 (m), 2878 (m), 2129 (s), 1489 (w), 1381 (m), 1358 (w), 1096 (s), 1072 (s), 1022 (m), 887 (m), 772 (s), 745 (s), 702 (s), 648 (m). $\mu_{eff} = 4.9(2) \mu B$ (calcd 4.9). Anal. Calcd for $C_{48}H_{64}N_2O_2Fe$: C, 76.2; H, 8.5; N, 3.7. Found: C, 76.1; H, 8.3; N, 3.8.

$(RO)Fe(THF)(\mu-NAr)_2Fe(THF)(OR)$ ($Ar = 4$ -trifluoromethylphenyl) (**5**). A 5.0 mL THF solution of 4-(trifluoromethyl)phenyl azide (14.1 mg, 0.075 mmol) was added dropwise to a 5.0 mL THF solution of **1** (48.1 mg, 0.075 mmol). Immediately gas evolution was observed, along with a solution color change to dark green. Over the course of a half hour the solution color gradually changed to black. The reaction was stirred for 4 h, upon which the volatiles were removed in vacuo to yield a black residue. Recrystallization from hexane at $-35^\circ C$ afforded the product as black crystals (9.2 mg, 48%). IR (cm^{-1}): 2963 (w), 2941 (w), 2880 (w), 1607 (w), 1489 (w), 1389 (w), 1319 (s), 1161 (m), 1107 (m), 1065 (s), 1015 (m), 839 (m), 745 (m), 706 (m). $\mu_{eff} = 3.81 \mu B$ (calcd 4.00). The compound was also characterized by X-ray crystallography. Anal. Calcd for $C_{50}H_{72}O_4N_2F_6Fe_2$: C, 61.7; H, 7.0; N, 2.8. Found: C, 61.3; H, 6.9; N, 3.0.

$(RO)Fe(THF)(\mu-NAr)_2Fe(THF)(OR)$ ($Ar = phenyl$) (**6**). A 5.0 mL THF solution of phenyl azide (7.7 mg, 0.065 mmol) was added dropwise to a 5.0 mL THF solution of **1** (41.3 mg, 0.065 mmol). Immediately gas evolution was observed, along with a solution color change to dark green. Over the course of a half hour the solution color gradually changed to a dark maroon. The reaction was stirred for 4 h, upon which the volatiles were removed in vacuo to yield a brown residue. Precipitation from hexane at $-35^\circ C$ afforded the product as a red-brown solid (7.4 mg, 52%). IR (cm^{-1}): 2920 (w), 2851 (w), 1520 (m), 1489 (w), 1462 (m), 1387 (m), 1119 (m), 1049 (s), 1016 (s), 968 (m), 845 (w), 721 (m), 710 (m). $\mu_{eff} = 4.51 \mu B$ (calcd 4.00). Anal. Calcd for $C_{32}H_{70}O_4N_2Fe_2$: C, 68.5; H, 8.3; N, 3.2. Found: C, 68.4; H, 8.1; N, 3.5.

$(RO)Fe(THF)(\mu-NAr)_2Fe(THF)(OR)$ ($Ar = 3,5$ -dimethylphenyl) (**7**). A 5.0 mL THF solution of 3,5-dimethylphenyl azide (10.4 mg, 0.0707 mmol) was added dropwise to a 5.0 mL THF solution of **1** (45.3 mg, 0.0709 mmol). Immediately gas evolution was observed, along with a solution color change to dark green. Over the course of a half hour the solution color gradually changed to a dark maroon. The reaction was stirred for 4 h, upon which the volatiles were removed in vacuo to yield a brown residue. Recrystallization from pentane at $-35^\circ C$ afforded the product as sticky brown crystals (7.3 mg, 44%). IR (cm^{-1}): 3003 (w), 2974 (w), 2938 (m), 2880 (m), 2833 (w), 1647 (w), 1593 (m), 1541 (w), 1506 (w), 1476 (s), 1435 (m), 1206 (m), 1140 (w), 1096 (m), 1049 (w), 1018 (s), 746 (s), 708 (w). $\mu_{eff} = 4.80 \mu B$ (calcd 4.00). The compound was also characterized by X-ray crystallography. Anal. Calcd for $C_{54}H_{80}O_4N_2Fe_2$: C, 69.5; H, 8.6; N, 3.0. Found: C, 68.0; H, 8.6; N, 1.9. The product was sticky and difficult to transfer in appreciable amounts. As such, satisfactory elemental analysis could not be obtained, even after repeated attempts.

Catalytic Conversion of Aryl Azides to Azoarenes. General Procedure for the Synthesis of Azoarenes. $Fe(OR)_2(THF)_2$ (25.0 mg, 0.039 mmol) (**1**) was dissolved in either THF or C_6D_6 in a scintillation vial. The aryl azide (~120–140 mg for 5 mol % of **1**) and the internal integration standard 1,3,5-trimethoxybenzene (65.0 mg, 0.39 mmol) were dissolved in the same solvent in a separate vial. The azide solution was then added dropwise to the solution of compound **1**, upon which gas evolution was observed, along with a gradual solution color change to red-orange. The reaction was stirred for the appropriate time (see Table S1), upon which NMR spectra were obtained for an aliquot of the solution, confirming complete consumption of the starting azide. The solution was then passed through a plug of silica to obtain the purified azoarene product, which

was massed to obtain a yield (see Table S1). The nature of the product was verified using mass spectrometry and 1H NMR spectroscopy.

Procedure for the Synthesis of Asymmetric Azoarenes. The same procedure as above (general procedure for the synthesis of azoarenes) was used, but an equal number of equivalents of both azides were first combined prior to dropwise addition to the catalyst. The reaction was stirred for the appropriate time, upon which NMR of an aliquot was taken. Mass spectrometry confirmed the presence of the asymmetric product for the reaction of mesityl azide and 2,6-diethylphenyl azide.

Control Experiments. Four separate control experiments were conducted. First, mesityl azide was stirred in the presence of iron(II) chloride and the internal standard for 24 h. NMR revealed that no reaction had taken place. Next, mesityl azide was stirred in the presence of iron(III) chloride and the internal standard for 24 h. NMR revealed that no reaction had taken place. Next, mesityl azide was stirred in the presence of the lithium salt of the ligand, LiOR, and the internal standard for 24 h. NMR revealed that no reaction had taken place. Finally, mesityl azide alone was stirred in the presence of the internal standard for 24 h. NMR revealed that no reaction had taken place.

Kinetics Experiments. 2,6-Diethylphenyl azide (628.2 mg, 3.59 mmol) and the internal standard 1,3,5-trimethoxybenzene (142.4 mg, 0.85 mmol) were dissolved in C_6D_6 . This solution was then added in one portion to a stirred solution of 1 mol % of **1** (22.9 mg, 0.036 mmol). NMR spectra of an aliquot of the solution were taken at regular intervals over a period of 7.5 h. The integration ratio with the standard was used to calculate the concentration of the azide, and its decrease was monitored. A plot of $1/[azide]$ vs time revealed a linear progression, suggesting that the catalysis is second order in azide (see Figures S31 and S32). Plots of the additional kinetics experiments using different concentrations of **1** and 2,6-diethylphenyl azide are given in Figures S33–35.

X-ray Crystallographic Details. The structures of **2**, **3**, **4**, **5**, and **7** were confirmed by X-ray analysis. The structure of **3** has been previously published.²⁷ The crystals were mounted on a Bruker APEXII/Kappa three-circle goniometer platform diffractometer equipped with an APEX-2 detector. A graphic monochromator was employed for wavelength selection of the Mo $K\alpha$ radiation ($\lambda = 0.71073 \text{ \AA}$). The data were processed, and the structure was solved using the APEX-2 software supplied by Bruker-AXS. The structure was refined by standard difference Fourier techniques with SHELXL (6.10 v., Sheldrick G. M., and Siemens Industrial Automation, 2000). Hydrogen atoms were placed in calculated positions using a standard riding model and refined isotropically; all other atoms were refined anisotropically.

Computational Details. Electronic structure calculations were carried out using DFT²⁸ as implemented in Gaussian09.²⁹ Geometry optimizations were performed at the B3LYP²⁰ level of theory using the 6-311G(d) basis set based on inadequacies we observed with double- ζ basis sets in a previous study.³⁰ No symmetry constraints were imposed during geometry optimizations. All optimized structures were confirmed to have stable wave functions³¹ and to be local minima by analyzing the harmonic frequencies.³² Cartesian coordinates, frequencies, and thermodynamics for all species may be found in Tables S5, S6, and S7.

■ ASSOCIATED CONTENT

Supporting Information

General methods and procedures, synthesis of all complexes, catalysis procedures, NMR, IR, UV–vis, and mass spectra, Evans data, X-ray crystallography, detailed catalytic data, detailed kinetics data, cif files for **2**, **3**, **5**, and **7**, and DFT calculation details. The Supporting Information is available free of charge on the ACS Publications website at DOI: 10.1021/acs.organomet.5b00231.

AUTHOR INFORMATION

Corresponding Author

*E-mail: groysman@chem.wayne.edu.

Notes

The authors declare no competing financial interest.

ACKNOWLEDGMENTS

We thank WSU and ACS PRF for the support of this work. We also thank Shervyn Karthanal and Katlyn Holt for technical assistance and Profs. Neal Mankad (UIC) and Stephen Matchett (GVSU) for helpful discussions. J.A.B. thanks WSU Graduate School for the Wilfred Heller Research Fellowship. Computational resources were provided by NSF-MRI award CHE-1039925 through the Midwest Undergraduate Computational Chemistry Consortium.

REFERENCES

- (1) Hunger, K. *Industrial Dyes: Chemistry, Properties, Applications*, 3rd ed.; Wiley-VCH: Weinheim, Germany, 2003.
- (2) Ashutosh, P. N. D.; Mehrotra, J. K. *Colourage* **1979**, *26*, 25.
- (3) Li, X. Y.; Wu, Y. Q.; Gu, D. D.; Gan, F. X. *Mater. Sci., Eng. B* **2009**, *158*, 53–57.
- (4) Ikeda, T.; Tsutsumi, O. *Science* **1995**, *268*, 1873–1875.
- (5) Feringa, B. L.; Van Delden, R. A.; Koumura, N.; Geertsema, E. M. *Chem. Rev.* **2000**, *100*, 1789–1816.
- (6) Roldo, M.; Barbu, E.; Brown, J. F.; Laight, D. W.; Smart, J. D.; Tsibouklis, J. *Expert Opin. Drug Delivery* **2007**, *4*, 547–560.
- (7) Merino, E. *Chem. Soc. Rev.* **2011**, *40*, 3835–3853.
- (8) Ray, K.; Heims, F.; Pfaff, F. F. *Eur. J. Inorg. Chem.* **2013**, 3784–3807.
- (9) (a) Hartwig, J. F. *Organotransition Metal Chemistry: From Bonding to Catalysis*; University Science Books: Mill Valley, CA, 2010. (b) Driver, T. G. *Org. Biomol. Chem.* **2010**, *8*, 3831–3846. (c) Eikey, R. A.; Abu-Omar, M. M. *Coord. Chem. Rev.* **2003**, *243*, 83–124. (d) Zhang, L.; Deng, L. *Chin. Sci. Bull.* **2012**, *57*, 2352–2360. (10) (a) Jenkins, D. M. *Synlett* **2012**, 1267–1270. (b) Fulton, J. R.; Holland, A. W.; Fox, D. J.; Bergman, R. G. *Acc. Chem. Res.* **2002**, *35*, 44–56. (c) Roizen, J. L.; Harvey, M. E.; Du Bois, J. *Acc. Chem. Res.* **2012**, *45*, 911–922. (d) Baidiei, Y. M.; Krishnaswamy, A.; Melzer, M. M.; Warren, T. H. *J. Am. Chem. Soc.* **2006**, *128*, 15056–15057. (e) Cowley, R. E.; DeYonker, N. J.; Eckert, N. A.; Cundari, T. R.; DeBeer, S.; Bill, E.; Ottenwaelder, X.; Flaschenriem, C.; Holland, P. L. *Inorg. Chem.* **2010**, *49*, 6172–6187. (f) Laskowski, C. A.; Miller, A. J. M.; Hillhouse, G. L.; Cundari, T. R. *J. Am. Chem. Soc.* **2011**, *133*, 771–773. (g) King, E. R.; Sazama, G. T.; Betley, T. A. *J. Am. Chem. Soc.* **2012**, *134*, 17858–17861. (h) King, E. R.; Hennessy, E. T.; Betley, T. A. *J. Am. Chem. Soc.* **2011**, *133*, 4917–4923. (i) Xiao, J.; Deng, L. *Dalton Trans.* **2013**, *52*, 5906–5913. (j) Zhang, H.; Ouyang, Z.; Liu, Y.; Zhang, Q.; Wang, L.; Deng, L. *Angew. Chem., Int. Ed.* **2014**, *53*, 8432–8436. (k) Zhang, L.; Liu, Y.; Deng, L. *J. Am. Chem. Soc.* **2014**, *136* (44), 15525–15528. (11) (a) Hansert, B.; Vahrenkamp, H. *J. Organomet. Chem.* **1993**, *459*, 265–269. (b) Harrold, N. D.; Waterman, R.; Hillhouse, G. L.; Cundari, T. R. *J. Am. Chem. Soc.* **2009**, *131*, 12872–12873. (c) Zarkesh, R. A.; Ziller, J. W.; Heyduk, A. F. *Angew. Chem., Int. Ed.* **2008**, *47*, 4715–4718. (12) (a) Ragaini, F.; Penoni, A.; Gallo, E.; Tollari, S.; Gotti, C. L.; Lapadula, M.; Mangioni, E.; Cenini, S. *Chem.—Eur. J.* **2003**, *9*, 249–259. (b) Mankad, N. P.; Müller, P.; Peters, J. C. *J. Am. Chem. Soc.* **2010**, *132*, 4083–4085. (c) Heyduk, A. F.; Zarkesh, R. A.; Nguyen, A. I. *Inorg. Chem.* **2011**, *50*, 9849–9863. (d) Takaoka, A.; Moret, M.-E.; Peters, J. C. *J. Am. Chem. Soc.* **2012**, *134*, 6695–6706. (13) (a) Bellow, J. A.; Fang, D.; Kovacevic, N.; Martin, P. D.; Shearer, J.; Cisneros, G. A.; Groysman, S. *Chem.—Eur. J.* **2013**, *19*, 12225–12228. (b) Bellow, J. A.; Martin, P. D.; Lord, R. L.; Groysman, S. *Inorg. Chem.* **2013**, *52*, 12335–12337. (14) (a) Cowley, R. E.; Elhaik, J.; Eckert, N. A.; Brennessel, W. W.; Bill, E.; Holland, P. L. *J. Am. Chem. Soc.* **2008**, *130*, 6074–6075. (b) Bonyhady, S. J.; Green, S. P.; Jones, C.; Nembenna, S.; Stasch, A. *Angew. Chem., Int. Ed.* **2009**, *48*, 2973–2977. (c) Bonyhady, S. J.; Jones, C.; Nembenna, S.; Stasch, A.; Edwards, A. J.; McIntyre, G. J. *Chem.—Eur. J.* **2010**, *16*, 938–955. (d) Gondzik, S.; Schulz, S.; Bläser, D.; Wölper, C.; Haack, R.; Jansen, G. *Chem. Commun.* **2014**, *50*, 927–929. (e) Fohlmeister, L.; Jones, C. *Aust. J. Chem.* **2014**, *67*, 1011–1016. (15) (a) Cantalupo, S. A.; Lum, J. S.; Buzzeo, M. C.; Moore, C.; DiPasquale, A. G.; Rheingold, A. L.; Doerrer, L. H. *Dalton Trans.* **2010**, *2*, 374–383. (b) Chambers, M. B.; Groysman, S.; Villagrán, D.; Nocera, D. G. *Inorg. Chem.* **2013**, *52*, 3159–3169. (16) (a) Clegg, W.; Sheldrick, G. M.; Stalke, D.; Bhaduri, S.; Khwaja, H. K. *Acta Crystallogr.* **1984**, *C40*, 2045–2047. (b) Link, H.; Decker, A.; Fenske, D. Z. *Anorg. Allg. Chem.* **2000**, *626*, 1567–1574. (c) Duncan, J. S.; Nazif, T. M.; Verma, A. K.; Lee, S. C. *Inorg. Chem.* **2003**, *42*, 1211–1224. (d) Takemoto, S.; Ogura, S.; Yo, H.; Hosokoshi, Y.; Kamikawa, K.; Matsuzaka, H. *Inorg. Chem.* **2006**, *45*, 4871–4873. (e) Duncan, J. S.; Zdilla, M. J.; Lee, S. C. *Inorg. Chem.* **2007**, *46*, 1071–1080. (f) Zdilla, M. J.; Verma, A. K.; Lee, S. C. *Inorg. Chem.* **2011**, *50*, 1551–1562. (g) Zhang, Q.; Xiang, L.; Deng, L. *Organometallics* **2012**, *31*, 4537–4543. (17) (a) Cenini, S.; Gallo, E.; Caselli, A.; Ragaini, F.; Fantauzzi, S.; Piangiolo, C. *Coord. Chem. Rev.* **2006**, *250*, 1234–1253. (b) Mehn, M. P.; Peters, J. C. *J. Inorg. Biochem.* **2006**, *100*, 634–643. (18) (a) Proulx, G.; Bergman, R. G. *J. Am. Chem. Soc.* **1995**, *117*, 6382–6383. (b) Fickes, M. G.; Davis, W. M.; Cummins, C. C. *J. Am. Chem. Soc.* **1995**, *117*, 6384–6385. (c) Barz, M.; Herdtweck, E.; Thiel, W. R. *Angew. Chem., Int. Ed.* **1998**, *37*, 2262–2265. (d) Albertin, G.; Antoniutti, S.; Baldan, D.; Castro, J.; Garcia-Fontan, S. *Inorg. Chem.* **2008**, *47*, 742–748. (e) Nieto, I.; Ding, F.; Bontchev, R. P.; Wang, H.; Smith, J. M. *J. Am. Chem. Soc.* **2008**, *130*, 2716–2717. (f) Ni, C.; Fetting, J. C.; Long, G. J.; Brynda, M.; Power, P. P. *Chem. Commun.* **2008**, 6045–6047. (g) Scepianiak, J. J.; Young, J. A.; Bontchev, R. P.; Smith, J. M. *Angew. Chem., Int. Ed.* **2009**, *48*, 3158–3160. (h) Moret, M.-E.; Peters, J. C. *Angew. Chem., Int. Ed.* **2011**, *50*, 2063–2067. (i) Searles, K.; Fortier, S.; Khusniyarov, M. M.; Carroll, P. J.; Sutter, J.; Meyer, K.; Mündiola, D. J.; Caulton, K. G. *Angew. Chem., Int. Ed.* **2014**, *53*, 14139–14143. (19) Hatanaka, T.; Miyake, R.; Ishida, Y.; Kawaguchi, H. *J. Organomet. Chem.* **2011**, *696*, 4046–4050. (20) (a) Vosko, S. H.; Wilk, L.; Nusair, M. *Can. J. Phys.* **1980**, *58*, 1200–1211. (b) Lee, C.; Yang, W.; Parr, R. G. *Phys. Rev. B* **1988**, *37*, 785–789. (c) Becke, A. D. *Phys. Rev. A* **1988**, *38*, 3098–3100. (d) Becke, A. D. *J. Chem. Phys.* **1993**, *98*, 1372–1377. (e) Stephens, P. J.; Devlin, F. J.; Chabalowski, C. F.; Frisch, M. J. *J. Chem. Phys.* **1994**, *98*, 11623–11627. (21) (a) Reiher, M.; Salomon, O.; Hess, B. A. *Theor. Chem. Acc.* **2001**, *107*, 48–55. (b) Salomon, O.; Reiher, M.; Hess, B. A. *J. Chem. Phys.* **2002**, *117*, 4729–4737. (c) Reiher, M. *Inorg. Chem.* **2002**, *41*, 6928–6945. (22) (a) Perdew, J. P.; Burke, K.; Ernzerhof, M. *Phys. Rev. Lett.* **1996**, *77*, 3865–3868. (b) Handy, N. C.; Cohen, A. J. *Mol. Phys.* **2001**, *99*, 403–412. (23) (a) Swart, M.; Groenhof, A. R.; Ehlers, A. W.; Lammertsma, K. *J. Phys. Chem. A* **2004**, *108*, 5479–5483. (b) Swart, M. J. *Chem. Theory Comput.* **2008**, *4*, 2057–2066. (24) Wiese, S.; Aguila, M. J. B.; Kogut, E.; Warren, T. H. *Organometallics* **2013**, *32*, 2300–2308. (25) Barral, K.; Moorhouse, A. D.; Moses, J. E. *Org. Lett.* **2007**, *9*, 1809–1811. (26) Laiter, D. S.; Mathison, C. J. N.; Davis, W. M.; Sadighi, J. P. *Inorg. Chem.* **2003**, *42*, 7354–7356. (27) Gabe, E. J.; Wang, Y.; Barclay, L. R. C.; Dust, J. M. *Acta Crystallogr. Sect. B* **1981**, *37*, 978–979. (28) Parr, R. G.; Yang, W. *Density-Functional Theory of Atoms and Molecules*; Oxford University Press: New York, 1989.

(29) Frisch, M. J.; Trucks, G. W.; Schlegel, H. B.; Scuseria, G. E.; Robb, M. A.; Cheeseman, J. R.; Scalmani, G.; Barone, V.; Mennucci, B.; Petersson, G. A.; Nakatsuji, H.; Caricato, M.; Li, X.; Hratchian, H. P.; Izmaylov, A. F.; Bloino, J.; Zheng, G.; Sonnenberg, J. L.; Hada, M.; Ehara, M.; Toyota, K.; Fukuda, R.; Hasegawa, J.; Ishida, M.; Nakajima, T.; Honda, Y.; Kitao, O.; Nakai, H.; Vreven, T.; Montgomery, J. A., Jr.; Peralta, J. E.; Ogliaro, F.; Bearpark, M.; Heyd, J. J.; Brothers, E.; Kudin, K. N.; Staroverov, V. N.; Keith, T.; Kobayashi, R.; Normand, J.; Raghavachari, K.; Rendell, A.; Burant, J. C.; Iyengar, S. S.; Tomasi, J.; Cossi, M.; Rega, N.; Millam, J. M.; Klene, M.; Knox, J. E.; Cross, J. B.; Bakken, V.; Adamo, C.; Jaramillo, J.; Gomperts, R.; Stratmann, R. E.; Yazyev, O.; Austin, A. J.; Cammi, R.; Pomelli, C.; Ochterski, J. W.; Martin, R. L.; Morokuma, K.; Zakrzewski, V. G.; Voth, G. A.; Salvador, P.; Dannenberg, J. J.; Dapprich, S.; Daniels, A. D.; Farkas, O.; Foresman, J. B.; Ortiz, J. V.; Cioslowski, J.; Fox, D. J. *Gaussian 09*, Revision D.01; Gaussian, Inc.: Wallingford, CT, 2010.

(30) Reed, B. R.; Stoian, S. A.; Lord, R. L.; Groysman, S. *Chem. Commun.* **2015**, *51*, 6496–6499.

(31) (a) Schlegel, H. B.; McDouall, J. J. In *Computational Advances in Organic Chemistry*; Oegretir, C.; Csizmadia, I. G., Eds.; Kluwer Academic: Amsterdam, The Netherlands, 1991. (b) Bauernschmitt, R.; Ahlrichs, R. *J. Chem. Phys.* **1996**, *104*, 9047–9052.

(32) (a) Schlegel, H. B. *J. Comput. Chem.* **1982**, *3*, 214–218.

(b) Schlegel, H. B. *WIREs Comput. Mol. Sci.* **2011**, *1*, 790–809.